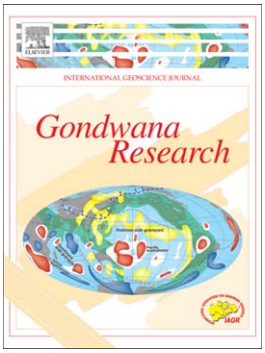

Reassessment of mid-Carboniferous glacial extent in southwestern Gondwana (Rio Blanco Basin, Argentina) inferred from paleo-mass transport of diamictites

Erik L. Gulbranson, John L. Isbell, Isabel P. Montañez, C. Oscar Limarino, Sergio A. Marenssi, Kyle Meyer, Clara Hull

PII: S1342-937X(13)00117-2
DOI: doi: 10.1016/j.gr.2013.03.017
Reference: GR 1029

To appear in: *Gondwana Research*

Received date: 2 May 2012
Revised date: 10 March 2013
Accepted date: 11 March 2013

Please cite this article as: Gulbranson, Erik L., Isbell, John L., Montañez, Isabel P., Limarino, C. Oscar, Marenssi, Sergio A., Meyer, Kyle, Hull, Clara, Reassessment of mid-Carboniferous glacial extent in southwestern Gondwana (Rio Blanco Basin, Argentina) inferred from paleo-mass transport of diamictites, *Gondwana Research* (2013), doi: 10.1016/j.gr.2013.03.017

Reassessment of mid-Carboniferous glacial extent in southwestern Gondwana (Rio Blanco Basin, Argentina) inferred from paleo-mass transport of diamictites

Erik L. Gulbranson[1,2†], John L. Isbell[2], Isabel P. Montañez[1], C. Oscar Limarino[3,4], Sergio A. Marenssi[3,4,5], Kyle Meyer[1], and Clara Hull[1]
[1]Department of Geology, University of California-Davis, One Shields Ave, Davis, CA, 95616, USA
[2]Department of Geosciences, University of Wisconsin-Milwaukee, Milwaukee, WI 53211, USA
[3]Department of Geology, University of Buenos Aires, Cuidad Universitaria, Pabellón II, 1428, Buenos Aires, Argentina
[4]Consejo Nacional de Investigaciones Cientificas y Técnicas (CONICET), Argentina
[5]Instituto Antártico Argentino, Cerrito 1248, C1010AAZ Buenos Aires, Argentina

Abstract

Late Paleozoic glacial diamictites occur in many localities in western Argentina, indicating that the region was strongly affected by glaciation during the mid-Carboniferous (late Serpukhovian-early Bashkirian). In most instances these diamictites are found in steeply walled paleovalley settings in the Andean Precordillera. This study presents new data from a locality north of the Precordillera that suggests an additional, distinct, volume of ice existed in the region during the Carboniferous. The glacigenic diamictites in the Rio Blanco Basin were ultimately emplaced as gravity flows, precluding inferences of paleo-ice volume. Fold nose orientation and soft-sediment groove orientations within the diamictites indicate that the deposits were emplaced from north to south, suggesting that glacial ice was most likely not sourced from the proto-Precordillera at this locality, requiring the need for another ice center to the north of the basin. Diamictite facies indicates that the sediment was initially supplied to the study area by a warm-based glacier.

Introduction

Late Paleozoic basins of northwestern Argentina contain a record of the mid-Carboniferous glaciation, primarily as diamictites containing faceted and striated clasts,

outsized clasts, diamictites resedimented via gravity flows, and evidence of subglacial erosion (Fig. 1; Lopez-Gamundí, 1987; 1992; Lopez-Gamundi and Martinez, 2000; Limarino et al., 2002; Pazos, 2002; Marenssi et al., 2005; Limarino and Spalletti, 2006; Henry et al., 2008; 2010; Gulbranson et al., 2010; Perez Loinaze et al., 2010). The majority of late Paleozoic glacigenic deposits in northwestern Argentina occur within steep-sided (~1000m) paleovalleys with the widespread occurrence of glacigenic and post glacial sediments on the southwestern margin of Gondwana implies a large volume of sediment being delivered to these paleovalleys (Fig. 1), consistent with interpretations of mass transport deposition in mid-Carboniferous diamictites throughout South America (Table 1). This study presents new evidence of mass transport deposition of glacigenic sediments during the late Paleozoic ice age in the Río Blanco Basin of northwestern Argentina. Although, resedimentation of these glacigenic sediments precludes inference of glacier size, the orientation of mass transport deposits argues for ice in the Río Blanco Basin, sourced from the north, independent of the well-known proto-Precordilleran glacial sources to the south and west (Fig. 1).

The Río Blanco Basin was a retro-arc basin that developed during the early Mississippian (Limarino et al., 2006) and contains a record of a Mississippian magmatic arc, glacial diamictites of the mid-Carboniferous glaciation, and paralic facies of late Pennsylvanian to early Permian age (Gulbranson et al., 2010). Provenance analysis of Carboniferous sedimentary rocks in the southern Rio Blanco Basin suggest sediment was transported from the proto-Precordillera and Sierras Pampeanas terrane to the south and east (Spalletti et al., 2012). The implication of a north-to-south transport direction reported herein is confirmation that a portion of the Río Blanco Basin was tectonically

distinct from the southern basins (cf., Limarino et al., 2002), and that there was likely a larger volume of glacial ice in the region of northwest Argentina than previously considered.

Outcrop-scale deformation of mid-Carboniferous diamictites in the Río Blanco Basin, as reported in other late Paleozoic basins throughout Argentina (Table 1), indicates that mass transport was a common depositional mechanism acting along the southwestern margin of Gondwana during the waning stages of the main glacial period (mid-Carboniferous) in southwestern Gondwana. The succession of diamictites presented in this paper highlights the complex nature of mass transport deposits, their internal structure and stratigraphic relationships, and presents evidence for mass transport over a spectrum of spatial scales (mm- to km-scale). Moreover the importance of mass transport of mid-Carboniferous glacigenic diamictites indicates that eustatic sea-level reconstructions based on inferences of ice volume from similar deposits are tenuous at best, given the limitations of inferring volume of glacial ice from such deposits presented in this study.

Stratigraphy of the Río Blanco Basin

The Río Blanco Basin of northwestern Argentina contains three primary stratigraphic units: the Angualasto Group, the Río del Peñon Formation of the Paganzo Gp., and the Choiyoi Gp. (Table 2; Fig. 2; Limarino and Spalletti, 2006). The Angualasto Gp. is Mississippian in age (Archangelsky et al., 1996), and is comprised of three stratigraphic units in the Río Blanco Basin: the Maliman, Cortaderas, and Punta del Agua fms (Fig. 2, Limarino and Spalletti, 2006). The Maliman Fm. is a coal-bearing unit comprised of shales and fine-grained sandstone interpreted as marine facies (Limarino

and Césari, 1993; Taboada and Shi, 2009). In contrast the upper Cortaderas Fm. is dominated by diamictites interpreted as glacigenic in origin (Perez Loinaze et al., 2010). The Maliman and Cortaderas fms directly overlie folded marine strata and pillow basalts of Devonian age indicating that the Maliman and Cortaderas fms record early Mississippian syn- and post-orogenic sedimentation (Fig. 2B). The Cortaderas Fm. in particular contains diamictite beds interpreted to be glacigenic in origin, which are dated to the Visean making these glacigenic deposits the oldest glacigenic succession in Argentina (Table 2; Gulbranson et al., 2010; Perez Loinaze et al., 2010). The Punta del Agua Fm. consists of interbedded conglomerate and andesite representing a volcanic arc that likely accreted during the late Mississippian Río Blanco orogenic episode (Limarino and Spalletti, 2006). ID-TIMS U-Pb ages on single zircon grains indicate that the uppermost Punta del Agua Fm. is Visean in age, 335.99 (± 0.06) Ma (Gulbranson et al., 2010).

The Río del Peñon Fm. overlies the Punta del Agua Fm. at the Río del Peñon locality (Fig. 2C), and consists of three members: lower, middle, and upper (Table 2; Scalabrini Ortiz, 1972). The lower Río del Peñon Fm. was considered to be Permian in age (Gonzalez and Bossi, 1986; Limarino et al., 1996), however, an ID-TIMS U-Pb age of 319.57 (± 0.09) Ma from a volcanic ash (Fig. 1D, Gulbranson et al., 2010) in the lower Rio del Peñon Fm. indicates that it is early Pennsylvanian (Bashkirian) in age. The stratigraphy of the lower Río del Peñon Fm. consists of sandstone and siltstone with carbonate concretions overlying andesite of the Punta del Agua Fm. (Table 2). Diamictites in the Río del Peñon Fm. were first described by Gulbranson et al. (2008) and include a succession of massive diamictite overlain by stratified diamictite that onlaps

onto the underlying Punta del Agua Fm. and is truncated by the overlying middle Río del Peñon Fm. in the study locality (Ezpeleta and Astini, 2008; Gulbranson et al., 2010). The contact between the middle and upper Río del Peñon Fm. is dated to the Pennsylvanian (Moscovian) based on an ID-TIMS U-Pb age of 310.63 (± 0.07) Ma from an ignimbrite (Gulbranson et al., 2010). The stratigraphy of the middle Río del Peñon Fm. consists of a thick succession of crossbedded sandstones and horizontally bedded siltstones deposited interpreted as fluvial sandstones (Table 2) and an overlying progradational shoreface succession containing invertebrate fauna of the *Tivertonia jachalensis-Streptorhynchus inaequiornatus* biozone (Taboada, 2010; Césari et al., 2011). Moreover, the invertebrate fauna in the Río Blanco Basin are unique from the southern basins (e.g., Tepuel Basin) because they contain warm water affinities as opposed to cold water fauna in the southern basins (Gonzalez, 1989; 1993; 1997). The upper Río del Peñon Fm. is no older than the Moscovian based upon the faunal association and U-Pb age of the middle Río del Peñon Fm. (Fig. 2D), and is composed of coarsening-upward and thickening-upward packages of laminated siltstones interbedded with sandstone and crossbedded multistory sandstones interpreted as a deltaic succession (Scalabrini Ortiz, 1972; Scalabrini Ortiz and Arrondo, 1973; Limarino et al., 1996).

Stratigraphic relationship of the Punta del Agua and Río del Peñon fms.

The contact between the Punta del Agua and Río del Peñon fms is irregular and represents an unconformity of significant duration (Figs. 2D, 3, 4). The unconformity is estimated to have a ~12 m.y.r. duration based on an ID-TIMS U-Pb zircon age of 319.57 Ma from an ash in the lower Río del Peñon Fm. (Gulbranson et al., 2010), a Serpukhovian (~324 Ma) age estimate for the base of the lower Río del Peñon Fm. based

on pollen and macroflora biostratigraphy (Perez-Loinaze, 2007; Balseiro et al., 2009; Césari et al., 2011), and the 335.99 Ma age from the uppermost Punta del Agua Fm. (Gulbranson et al., 2010). In the study area the nature of this contact suggests that the lower Río del Peñon Fm. was deposited in a valley-style topography, which can be observed on the northern end of the syncline (Fig. 4A), and is implied by the lateral discontinuity of the lower Río del Peñon Fm. (Fig. 3B). At the outcrop-scale the contact between the Punta del Agua and Río del Peñon fms is highly irregular (Figs. 3, 4B). In certain areas, stratified diamictite rests directly on the Punta del Agua Fm. andesite and the basal-most massive diamictites are absent. The nature of this contact implies that the Punta del Agua Fm. formed a pre-existing topography with tens of meters of relief that influenced the deposition of the lower Río del Peñon Fm. (Figs. 3B, 4).

Lower Río del Peñon Formation

Basal diamictites

Diamictites of the lower Río del Peñon Fm. contain predominantly andesitic clasts and boulders with minor amounts of granitic clasts, and the matrix is composed of lithic fragments and subangular quartz grains. Metamorphic rocks and sandstone clasts are rare. Clast sorting is poor, but a few discrete layers exhibit normal grading (Gulbranson et al., 2008). The basal diamictites are massive and matrix-supported, but transition to stratified and matrix-supported diamictite towards the uppermost portion of the lower Río del Peñon Fm. Despite the lack of internal structure of the diamictites, some bedding planes exhibit elongate non-parallel curvilinear grooves that display an asymmetric profile (Fig. 5). These grooved surfaces grade laterally into non-grooved surfaces.

Lithic sandstones are interbedded within the massive basal diamictites. These sandstones are either massive or current ripple cross-stratified. The sandstones are laterally discontinuous, and extend laterally between 2m and 4m in width. In some cases outsized clasts penetrate the upper surface of these sandstones beds.

Interpretation of basal diamictite

The massive structure of the diamictite suggests that it formed as a debris flow deposit. However, the curvilinear grooves on bedding planes are consistent with iceberg-keel marks as suggested by the asymmetric groove geometry and the observation that the grooves laterally transition to unmodified surfaces (Fig. 5, cf., Woodworth-Lynas and Dowdeswell, 1994). Mass transport deposition can also form soft-sediment grooves, however, the curvilinear form of the grooves and irregular boundaries suggest unique and independent pathways plowed into the sediment by an uneven object, which is suggestive of iceberg-keels. Moreover, stratified diamictites directly overlie the grooved surface, implying that ice-rafted debris was associated closely in time with the grooved surface. The presence of iceberg-keel marks strongly suggests a glacial affinity for the diamictite and that the debris flow deposits were formed as part of an outwash fan due to its massive structure. The stratified diamictite at the top of the unit was likely formed as a continuum of suspension settling from meltwater plumes and clasts deposited from icebergs or sea ice, which explains the bimodal grain distribution (Thomas and Connell, 1985; Powell and Domack, 2002).

Massive and ripple-laminated sandstones intercalated within the diamictite are interpreted as grounding line fan sediment deposited downstream of a turbulent subglacial jet (Powell, 1990; Powell and Domack, 2002). The ripple-laminated portion of

the sandstone likely formed in the upstream portion of the fan, and was subjected to centimeter-scale scouring. The downstream portion of the fan is dominated by massive sandstone, suggesting sandy debris flow on the lee-side of the structure. Moreover, the massive sandstone is partially truncated by diamictite, suggesting that rainout from debris-laden icebergs impacted this feature (cf., Lisitzin, 2002).

Outcrop-scale sediment structures

Decimeter to meter-scale slip-planes, folds, and back-tilted strata indicate that the complex arrangement of outwash fans, dunes, turbidity flows and debris flows were transported after deposition, as a coherent mass, and thus represent a secondary control on sediment deposition of the basal diamictites of the lower Río del Peñon Fm. To constrain these features in space, four outcrops of diamictite were studied along a N-S trending out cropping of the Rio del Peñon Fm. north of route 76 near a prominent construction campsite, west of the village of Jagüel, La Rioja province (Figs. 3, 6). Diamictite outcrops at section 1 and 2 do not show evidence of internal deformation and display similar strike and dip as the overlying middle Río del Peñon Fm. (Fig. 6). Diamictites at section 3 exhibit changes in bedding geometry at the ~100 meter-scale, with basal diamictite and a sandstone body showing dip changes of ~10º relative to the overlying middle Río del Peñon Fm. Diamictites at section 4 exhibit a complex arrangement of at least five packages of diamictite and sandstone, with four of these packages displaying intense deformation. Diamictite in contact with the Punta del Agua Fm. at section 4 does not exhibit deformation features, but curvilinear grooves occur on some bedding planes of this basal-most diamictite. Directly overlying this grooved surface is the first of four internally deformed diamictite packages at section 4.

The succession of diamictite at section 3 displays bedding planes that oversteepens towards the southeast, towards the contact with the Punta del Agua Fm. (Fig. 7). The basalmost diamictite at section 3 displays similar dip direction and strike as the underlying Punta del Agua Fm. and does not display evidence of shearing or folding. The diamictite overlying the basal-most diamictite is divided into three distinct packages on the basis of fold geometries and noticeable changes in dip angle. Each of these three diamictite packages are internally deformed with the lower two packages showing pronounced folding (Fig. 7) and the upper diamictite displaying minor folding and uptilting of strata. In addition the lowermost diamictite ('diamictite1', Fig. 7) contains two large (>5m) blocks of andesite that are positioned along strike from the folded region of this diamictite. The fact that these three diamictite packages display intense folding and dip angle changes in contrast to the overlying sandstones of the middle Río del Peñon Fm., that does not exhibit such deformation, indicates that the diamictite succession was internally deformed soon after deposition (Fig. 7).

In addition to the meter-scale deformation features, centimeter-scale structures are observed in intensely sheared intervals that occur in the contact between the two folded diamictites. A granitic clast (2.5 cm b-axis, 4.3 cm a-axis) is found at the contact between the sheared interval and the lowermost folded diamictite. This clast is surrounded on either side by moderately sorted medium- to coarse-grained sandstone that pinch-out <1cm away from the granite clast. Finely laminated green siltstone underlies this clast and is upturned on one side of the granite clast. In addition, lenses of poorly sorted coarse-grained sandstone occur within the red moderately sorted arkosic sandstone that surrounds the granite clast, these lenses exhibit a conspicuous sigmoidal shape.

Overlying the granite clast is a ~3cm thick interval of sandstone "micro-thrusts" (Fig. 8). The sandstone micro-thrusts occur in an olive-colored poorly sorted lithic arkose sandstone and are identified as being three discrete red moderately sorted arkose sandstone blocks that are upturned in an en echelon trend. The olive-colored sandstone exhibits flame structures adjacent to these micro-thrusts.

Diamictites at section 4 exhibit large-scale thrusts and deformation that define five separate packages of diamictite. The first package of diamictite does not display evidence of internal deformation, however, this diamictite ('diamictite 1', Fig. 9) abuts upward against the second package of diamictite ('diamictite 2', Fig. 9), resulting in a vertical orientation of the bedding. The second package of diamictite exhibits oversteepened bedding geometry within the diamictite and an irregular contact with the underlying diamictite. The third and fourth diamictite packages are undeformed ('diamictite 3', 'diamictite 4', Fig. 9), and have bedding geometries consistent with the overall strike and dip of the Lower and Middle members of the Río del Peñon Fm. The fifth diamictite ('diamictite 5', Fig. 9) displays evidence of thrusts at the contact with the underlying diamictites. Upsection, interbedded sandstones in the fifth diamictite are back-tilted and offset by meter-scale thrust and reverse thrust faults. Isolated soft sediment grooves occur on the top of some of the deformed diamictite packages. These grooves occur in decimeter- to meter-scale patches that pass into unmodified surfaces.

Interpretation of large-scale sedimentary structures

Deformation of diamictites at section 3 indicates that after the diamictites were deposited from outwash fans and plumes, large amounts of diamictite were displaced and transported, presumably downslope, resulting in intense folding and shearing during

transport. At least three intervals of mass movement are recorded at section 3 (Fig. 7), the first is the thinner section of folded diamictite that contains blocks of andesite ('diamictite 1'), a second package consisting of a thick diamictite that is intensely folded ('diamictite 2'), and a third package of diamictite displaying minor folding and upturned beds ('diamictite 3'). Such deformation in sedimentary packages can be created by subglacial processes or through mass movement (Le Heron et al., 2005; Shanmugam, 2006). Beneath warm-based glaciers such deformation would be accompanied by extensive soft-sediment striations and grooves or formation of either a glacitectonite or deformation till, since the ice and sediment would only be partially coupled. The unfrozen sediment would be allowed to slip, creating an asymmetric strain zone with the development of fissility that would be the manifestation of intense shearing. Beneath a cold-based glacier deformation would extend from the subglacial sediment and into the overriding ice (Huddart and Hambrey, 1996; Van Der Wateren, 2002; Le Heron et al., 2005). The folding at section 3 suggests that at least two décollements are present (Fig. 7), indicating that deformation would have been partially uncoupled from an overriding glacier. Therefore we reject the hypothesis that a cold-based glacier overrode these diamictites. In contrast, shearing and folding are consistent with deformation of a warm-based glacier partially coupled to the underlying sediment (Le Heron et al., 2005). Soft-sediment grooves that are expected to develop from such deformation were observed in the uppermost portion of the deformed diamictites, suggesting possible deformation by an overriding glacier. The fact that the soft-sediment grooved sandstone is not, in-turn, overlain by glacigenic diamictite makes an interpretation of glacial affinity for these grooves tenuous, as they can also be produced on glide planes of slump and slide blocks.

Moreover, the discontinuous nature of shearing and folding between the three diamictite packages would suggest that three individual ice advance events created the deformation. However, no evidence of ice advance (striations, lodgment till) was observed in between the diamictite packages. Thus, deformation of these diamictites in a subglacial environment is equivocal since such deformation can also occur during mass transport (Shanmugam, 2006).

While gravity-driven processes (e.g., debris flows, turbidity currents) are likely responsible for much of the meter-scale diamictite packages, large-scale gravity driven processes such as slumps or slide blocks were likely important in defining the succession of decimeter- to meter-scale diamictite packages in the study area. Slumps are internally folded and brecciated during transport, whereas slides are not internally deformed, and these features are largely related to rotational or translational transport mechanisms, respectively (Shanmugam, 2006). The folding and shearing observed at section 3 is indicative of ductile or plastic deformation and is consistent with rotational mass transport. Thus, the diamictite succession at section 3 is interpreted as a series of slump or slide blocks (Fig. 7).

The granite clast and surrounding sediment at section 3 are interpreted as an augen-type clast that formed from the *in situ* rotation of the clast within the sediment under a low stress environment. The surrounding sandstone is analogous to pressure-shadows since they are widest nearest the clast and pinch-out within <1cm from the granite clast. The orientation of this shearing is measured at 163º. The overlying sandstone micro-thrusts also display a 163º orientation and are interpreted as resulting from shearing of unconsolidated sediment with variable pore-water pressure. The brittle-

style deformation of the red sandstone and dewatering features in the olive-colored sandstone imply different rheology between the two sandstones that would result in different responses to stress. Thus, the 'micro thrusts' observed at section 3 (Fig. 8) are likely the manifestation of shearing along a glide plane during the transport of the diamictite slump/slide deposit.

In contrast to the predominantly ductile style of deformation at section 3, diamictites at section 4 are interpreted as exhibiting brittle deformation. The lowermost deformed diamictite displays an erosive basal contact, and underlying sediments are observed to wrap around this diamictite (Fig. 9), features that are consistent with rapid emplacement of a consolidated mass of sediment into an unlithified substrate. Conversely, it is possible that the diamictite at section 4 represents the down-dip portion of a slump block and the outcrop at section 4 only displays the toe thrusts of slump block. Thrust faults with an orientation of between 110º and 150º occur near the basal contact of the uppermost diamictite, reflecting the accumulation of strain within the diamictite during compressive deformation. Sandstone is interbedded with the uppermost diamictite, and this sandstone displays both thrust faults and reverse faults (back-tilting), consistent with the thrust faults developed below (Fig. 9). Similar to section 3, the diamictites at section 4 lack evidence suggesting they were deformed in a subglacial environment. The brittle deformation observed at section 4 suggests that the primary difference between diamictite deformation at sections 3 and 4 is that section 3 accumulated strain over a period of time, and section 4 accumulated strain instantaneously. The difference in accumulated strain indicates that diamictite at section 3 was transported over a longer distance, whereas diamictite at section 4 was not only transported over a short distance,

but also likely encountered the local paleotopographic high of the underlying Punta del Agua Fm. during the transport of the diamictite. The diamictite at section 4 is laterally continuous for ~10 to 15 m, where it is bounded to the north and south by andesite of the Punta del Agua Fm., therefore, it is likely that the andesite provided a rigid obstacle during the emplacement of the uppermost diamictite resulting in instantaneous deformation of the mass transport deposit.

Discussion

Basal diamictites of the lower Río del Peñon Fm. have been interpreted as having a glacial affinity (Gulbranson et al., 2008). This work builds upon that interpretation with new field-based evidence for mass transport and emplacement of glacigenic diamictites found at the Río del Peñon locality (cf. Table 2). Therefore, while some aspects of the diamictite succession are of glacial affinity (e.g., grooves, dropstones), the majority of the succession was deposited as mass transport deposits. In other words, a significant portion of the basal diamictite of the lower Río del Peñon Fm. is interpreted as resedimented glacigenic diamictite. For the following discussion it is assumed that mass transport deposition of glacigenic diamictite will occur, generally, in the opposite direction from a retreating glacier. The orientation of mass transport deposition is NW-SE based on orientation measurements of shear planes and thrust faults interpreted to have formed during gravity flows. This transport direction is inconsistent with glacial advance from the proto-Precordillera or Sierras Pampeanas, which would result in expected orientations of S/SE-N/NW. Therefore, the resedimented glacigenic diamictites at the Río del Peñon locality were likely sourced from a distinct glaciated region in the northern Río Blanco Basin during the mid-Carboniferous.

The age range of the basal diamictites at Río del Peñon is between 319 Ma and 324 Ma as determined by U-Pb ages on volcanic ashes within the succession (Gulbranson et al., 2010) and regional correlations between fossil flora (César et al., 2011). This age is equivalent to glacigenic diamictites in the Paganzo Basin and Calingasta-Uspallata Basin of Argentina (Henry et al., 2008; 2010; Gulbranson et al., 2010), and correlative to the mid-Carboniferous glacigenic diamictites of eastern Australia (glacial interval "C2" of Fielding et al., 2008). The synchrony of these glacigenic strata implies that they reflect a global icehouse climate during the mid-Carboniferous in discrete regions of the supercontinent of Gondwana, and this inference is supported by a major eustatic fall observed in the U-Pb calibrated stratigraphy of the Donets Basin of eastern Ukraine (Eros et al., 2012a; 2012b) and elsewhere (Haq and Schutter, 2008). The mass transport deposits of the Río del Peñon Formation do indicate that large volumes of sediment, initially glacially influenced, were delivered to the marine margin of Gondwana during the mid-Carboniferous and that similar and time equivalent sediment gravity flow processes occurred throughout the Precordillera region of Argentina (Table 1; Kneller et al., 2004; Dykstra et al., 2006; Henry et al., 2008). The widespread occurrence of mass transport deposits in northwestern Argentina suggests that glacigenic sediments in the region were deposited under similar circumstances, such as high sediment influxes on steep slopes. In turn, we speculate that for the aforementioned reasons glaciation in the region was driven by the uplift of mountain ranges (e.g., the Protoprecordillera) along the southwestern margin of Gondwana during the mid-Carboniferous, providing high relief, sediment source areas, and the elevation of the land surface above the equilibrium line altitude (Isbell et al., 2012).

The contact between the Punta del Agua and Lower Río del Peñon fms delineates a valley-like topography that existed prior to deposition of Lower Río del Peñon Fm. This topography was highly irregular including a paleotopographic high that separated depositional areas now recorded at sections 3 and section 4 (Figs. 3, 4). Section 1 displays a slightly different succession of diamictites than the other sections at the study locality, suggesting that the position within the paleovalley influenced the occurrence of mass transport deposition. The facies and lack of deformation features at section 1 indicate correlation to the uppermost portion of the diamictite succession at section 2 (Fig. 5), suggesting highly variable thickness (10m and 20m) of diamictite deposits along the paleotopography, with maximum accumulation of diamictite in section 3. The large thickness of diamictite at section 3 implies increased accommodation space for sediment accumulation relative to the other sections. An increase in rate of development of accommodation space due to ice loading provides a plausible explanation for ductile deformation at this locality versus brittle deformation in the narrower, more spatially restricted portion of the paleovalley at section 4 (Figs. 3, 4), a conclusion further supported by the occurrence of soft-sediment grooves at the top of the diamictite succession at section 3 that suggest deformation by an overriding glacier or by mass transport.

Iceberg-keel marks (Fig. 5) indicate that the glacier(s) was grounded below sea-level and actively calved icebergs into the depositional basin. Regionally, late Paleozoic diamictites have been interpreted as derived from warm-based glaciers in the Proto-precordilleran area of Argentina (Table 1; López-Gamundí and Martinez, 2000; Marenssi et al., 2005; Henry et al., 2008; 2010). Moreover the glaciers in the Proto-precordilleran

region are interpreted to be alpine in nature, discrete, and of small ice volume. While we cannot determine the size of the glacier that fed sediment to the study location, the warm-based thermal character of the ice is consistent with warm-based glacier settings inferred from morainal bank complexes (Marenssi et al., 2005), high sediment yields, occurrence of glacigenic strata within paleovalleys, and deformation of glacigenic diamictite (Kneller et al., 2004; Dykstra et al., 2006; Henry et al., 2008) on the southwestern margin of Gondwana and may suggest that the glacial ice flow was rapid in this region.

Conclusions

Mid-Carboniferous diamictites of the Río Blanco Basin, northwest Argentina, record large-scale brittle and ductile deformation that is interpreted to have formed through subglacial processes and mass transport deposition. Thick accumulation of diamictite interstratified with ripple-laminated sandstone contain outsized clasts indicates that the basal diamictites were initially deposited in front of a warm-based glacier near the study area. The complex nature of the diamictite beds, which display sheared fabric, glide planes, and thrust faults suggests that the glacigenic diamictite underwent mass transport in a confined and uneven paleovalley setting. The evidence of mass transport indicates that large volumes of sediment were delivered to the Río Blanco Basin during the mid-Carboniferous glaciation similar to mass transport deposits described elsewhere in Argentina. The N-S transport direction of these mass flow deposits requires a glaciated source area in the Río Blanco Basin distinct from the proto-Precordillera to the west. These results suggest that the alpine style glacial centers previously interpreted for this region of southwestern Gondwana during the latest Mississippian to earliest Pennsylvanian may have been more extensive than previously considered. The volume

and area of this additional ice source, however, cannot be constrained from the basal diamictites of the Río Blanco Basin since displacement of the diamictite during mass transport overprints via displacement, rotation, and faulting characteristics useful for ice volume reconstruction such as paleo-ice flow direction from subglacial scouring and erosion, and depositional setting such as the paleo-fjords interpreted from the Precordillera region of Argentina. While the basal diamictite of the Río Blanco Basin occurs within a paleovalley, there is insufficient evidence that this late Paleozoic valley was formed by glacial erosion or modified by glacial erosion, characteristics expected from a warm-based glacier.

Acknowledgements

This manuscript benefitted from the critical and thoughtful reviews of Markus Aretz and Arturo Taboada, two anonymous reviewers and Editor Zhong Chen. This work was supported by funding from NSF grants OISE-0826105, EAR-05545654, and EAR-0650660 to the University of California-Davis, and NSF grants OISE-0825617, OPP-0943935, OPP-0944532, and ANT-1142749 to the University of Wisconsin-Milwaukee.

References

Archangelsky, S., Azcuy, C.L., César, S., González, C., Hünicken, M., Mazzoni, A., and Sabattini, N., 1996. Correlación y edad de las biozonas. In: Archangelsky, S. (Ed.) El Sistema Pérmico en la República Argentina y en la República Oriental del Uruguay, Academia Nacional de Ciencias Córdoba, Argentina, p. 203-226.

Atkins, C.B., Barrett, P.J., Hicock, S.R., 2002. Cold glaciers do erode and deposit: evidence from Allan Hills, Antarctica. Geology, v. 30, p. 659-662.

Balseiro, D., Rustán, J.J., Ezpeleta, M., Vaccari, N.E., 2009. A new Serpukhovian (Mississippian) fossil flora from western Argentina: paleoclimatic, paleobiogeographic, and stratigraphic implications. Palaeogeography, Palaeoclimatology, Palaeoecology, v. 280, p. 517-531.

Benn, D.I., and Evans, D.J.A., 2010. Glaciers and Glaciation. Hodder Education, Oxon, U.K., 802 pp.

Césari, S.N., Limarino, C.O., and Gulbranson, E.L., 2011. An Upper Paleozoic bio-chronostratigraphic scheme for the western margin of Gondwana. Earth-Science Reviews, v. 106, p. 149-160.

Domeier, M., Van Der Voo, R., Tohver, E., Tomezzoli, R.N., Vizan, H., Kirshner, J., 2011. New Late Permian paleomagnetic data from Argentina: refinement of the apparent polar wander path of Gondwana. Geochemistry, Geophysics, Geosystems, v. 12, p. 1-21.

Dykstra, M., Kneller, B., and Milana, J.P., 2006. Deglacial and postglacial sedimentary architecture in a deeply incised paleovalley-paleofjord; the Pennsylvanian (late Carboniferous) Jejenes Formation, San Juan, Argentina. GSA Bulletin, v. 118, p. 913-937.

Eros, J.M., Montañez, I.P., Osleger, D.A., Davydov, V.I., Nemyrovska, T.I., Poletaev, V.I., Zhykalyak, M.V., 2012a. Sequence stratigraphy and onlap history of the Donets Basin, Ukraine: insight into Late Paleozoic Ice Age dynamics. Palaeogeography, Palaeoclimatology, Palaeoecology, v. 313-314, p. 1-25.

Eros, J.M., Montañez, I.P., Davydov, V.I., Osleger, D.A., Nemyrovska, T.I., Poletaev, V.I., Zhykalyak, M.V., 2012b. Reply to the comment on "Sequence stratigraphy and onlap history of the Donets Basin, Ukraine: insight into Carboniferous icehouse dynamics". Palaeogeography, Palaeoclimatology, Palaeoecology, v. 363-364, p. 187-191.

Espejo, I.S., Lopez-Gamundi, O.R., 1994. Source versus depositional controls on sandstone composition in a foreland basin: the El Imperial Formation (mid Carboniferous-Lower Permian), San Rafael Basin, western Argentina. Journal of Sedimentary Research, Section A: Sedimentary Petrology and Processes, v. 64A, p. 8-16.

Ezpeleta, M., Astini, R.A., 2008. Labrado y relleno de un paleovalle glacial en la base de la Formación Río del Peñón (Carbonífero Superior), Precordillera Septentrional (La Rioja, Argentina). 5º Simposio Argentino del Paleozoico Superior (MACN, 2008), Resúmenes, p. 17.

González, C.R., 1989. Relaciones bioestratigráficas y paleogeográficas del Paleozoico superior marino en el Gondwana sudamericano. Acta Geológica Lilloana (Tucumán), v. 17, p. 5-20.

González, C.R., 1993. Late Paleozoic faunal succession in Argentina.In Compte Rendu XII International Congress on Carboniferous and Permian Stratigraphy and Paleontology, Buenos Aires, 1991, ed. S. Archangelsky.

González, C.R., 1997. Upper Palaeozoic glaciation and Carboniferous and Permian faunal changes in Argentina. In Late Paleozoic and Early Mesozoic circum-Pacific events and their global correlation. World and Regional Geology, v. 10, eds. J.M. Dickin, Yang Zunyi, Yin Hongfu, S.G. Lucas, S.K. Acharyya, Cambridge University Press, Cambridge, UK 243 pp.

González, C.R., Bossi, G.E., 1986. Los depósitos carbónicos al oeste du Jagüel, La Rioja. In Actas IV Congeso Argentino de Paleontologia y Bioestratigrafia, Mendoza, v. 1, p. 231-236.

González-Bonorino, G., 1992. Carboniferous glaciation in Gondwana. Evidence for grounded marine ice and continental glaciation in aouthwestern Argentina. Palaeogeography Palaeoclimatology, Palaeoecology, v. 91, p. 363-375.

Gulbranson, E.L., Limarino, C.O., Marenssi, S., Montañez, I., Tabor, N.J., Davydov, V., and Colombi, C., 2008. Glacial deposits in the Río del Peñon Formation (Late Carboniferous), Río Blanco Basin, northwestern Argentina. Latin American Journal for Sedimentology and Basin Analysis, v. 15, p. 129-142.

Gulbranson, E.L., Montañez, I.P., Schmitz, M.D., Limarino, C.O., Isbell, J.L., Marenssi, S.A., and Crowley, J.L., 2010. High-precision U-Pb calibration of Carboniferous glaciation and climate history, Paganzo Group, NW Argentina. GSA Bulletin, v. 122, p. 1480-1498.

Gulbranson, E.L., 2011. Paleoclimate reconstruction of the Paganzo and Río Blanco basins, NW Argentina. PhD dissertation. University of California, Davis, 204 p.

Gutiérrez, P.R., Limarino, C.O., 2006. El perfil del sinclinal del Rincón Blanco (noroeste de La Rioja): el límite Carbonifero-Pérmico en el noroeste argentino. Ameghiniana, v. 43, p. 687-703.

Haq, B.U., Schutter, S.R., 2008. A chronology and Paleozoic sea-level changes. Science, v. 322, p. 64-68.

Henry, L.C., Isbell, J.L., and Limarino, C.O., 2008. Carboniferous glacigenic deposits of the Protoprecordillera of west central Argentina. In: Fielding, C.R., Frank, T.D., and Isbell, J.L. (Eds.), Resolving the Late Paleozoic Ice Age in Time and Space, Geological Society of America Special Paper 441, p. 131-142.

Henry, L.C., Isbell, J.L., Limarino, C.O., McHenry, L.M., and Fraiser, M.L., 2010. Mid-Carboniferous deglaciation of the Protoprecordillera, Argentina recorded in the Agua de

Jagüel paleovalley. In: Shi, G. (Eds.), Palaeogeography, Palaeoclimatology, Palaeoecology special volume: High Latitudes.

Huddart, D., and Hambrey, M.J., 1996. Sedimentary and tectonic development of a high arctic, thrust-moraine complex: Comfortlessbreen, Svalbard. Boreas, v. 25, p. 227-243.

Kneller, B., Milana, J.P., Buckee, C., and Al Ja'aidi, O.S., 2004. A depositional record of deglaciation in a paleofjord (late Carboniferous [Pennsulvanian] of San Juan Province, Argentina); the role of catastrophic sedimentation: GSA Bulletin, v. 116, p. 348-367.

Le Heron, D.P., Sutcliffe, O.E., Whittington, R.J., and Craig, J., 2005. The origins of glacially related soft-sediment deformation structures in Upper Ordovician glaciogenic rocks: implication for ice-sheet dynamics. Palaeogeography, Palaeoclimatology, Palaeoecology, v. 218, p. 75-103.

Limarino, C.O., Césari, S.N., 1993. Reubicación estratigráfica de la Formación Cortaderas y definición del Grupo Angualasto (Carbonífero Inferior, Precordillera de San Juan). Revista de la Asociación Geológica Argentina, v. 47, p. 61-72.

Limarino, C.O., Césari, S.N., Net, L.I., Marenssi, S.A., Gutierrez, R.P., and Tripaldi, A., 2002. The Upper Carboniferous postglacial transgression in the Paganzo and Río Blanco basins (northwestern Argentina): facies and stratigraphic significance. Journal of South American Earth Sciences, v. 15, p. 445-460.

Limarino, C.O., and Spalletti, L.A., 2006. Paleogeography of the upper Paleozoic basins of southern South America: An overview. Journal of South American Earth Sciences, v. 22, p. 134-155.

Lisitzin, A.P., 2002. Sea-ice and iceberg sedimentation in the ocean. Springer-Verlag, Berlin.

López-Gamundí, O.R., 1987. Depositional models for the glaciomarine sequences of Andean Late Paleozoic basins of Argentina. Sedimentary Geology, v. 52, p. 109-126.

López-Gamundí, O.R., Limarino, C.O., Césari, S.N., 1992. Late Paleozoic paleoclimatology of central west Argentina. Palaeography, Palaeoclimatology, Palaeoecology, v. 91, p. 305-329.

López-Gamundí, O.R., and Martinez, M., 2000. Evidence of glacial abrasion in the Calingasta-Uspallata and western Paganzo Basins, mid-Carboniferous of western Argentina. Palaeogeography, Palaeoclimatology, Palaeoecology, v. 159, p. 145-165.

Marenssi, S.A., Tripaldi, A., Limarino, C.O., and Caselli, A.T., 2005. Facies and architecture of a Carboniferous grounding-line system from the Guandacol Formation, Paganzo Basin, northwestern Argentina. Gondwana Research, v. 8, p. 187-202.

NASA Landsat Program, 2002. Landsat ETM+ scene WSR-2, path 232, row 080, Orthorectified/Geocover, USGS, Sioux Falls, 02/10/2012.

Pazos, P.J., 2002. The late Carboniferous glacial to postglacial transition: facies and sequence stratigraphy, western Paganzo Basin, Argentina. Gondwana Research, v. 5, p. 467-487.

Perez Loinaze, V.S., Limarino, C.O., and Césari, S.N., 2010. Glacial events in Carboniferous sequences from Paganzo and Río Blanco basins (northwest Argentina): palynology and depositional setting. Geologica Acta, v. 8, p. 399-418.

Powell, R.D., 1990. Glacimarine processes at grounding-line fans and their growth to ice contact deltas. In: Dowdeswell, J.A. and Scourse, J.D. (Eds.) Glacimarine Environments: processes and sediments, Geological Society Special Publication, London, p. 53-73.

Powell, R., and Domack, E., 2002. Modern glaciomarine environments. In: Menzies J. (Ed.) Modern and past glacial environments, revised student edition. Butterworth-Heinemann Ltd., Oxford, p. 361-389.

Rocha-Campos, A.C., dos Santos P.R., Canuto, J.R., 2008. Late Paleozoic glacial deposits of Brazil: Paraná Basin. In: Fielding, C.R., Frank, T.D., and Isbell, J.L. (Eds.), Resolving the Late Paleozoic Ice Age in Time and Space, Geological Society of America Special Paper 441, p. 97-114.

Scalabrini Ortiz, J., 1972. Carbónico en el sector septentrional de la Precordillera sanjuanina. Revista de la Asociación Geológico Argentino. Actas II, 89-103.

Shanmugam, G., 2006. Deep-water processes and facies models: implications for sandstone petroleum reserves. Elsevier, Amsterdam, 476 pp.

Spalletti, L.A., Limarino, C.O., Piñol, F.C., 2012. Petrology and geochemistry of Carboniferous siliciclastics from the Argentine Frontal Cordillera: a test of methods for interpreting provenance and tectonic setting. Journal of South American Earth Sciences, v. 36, p. 32-54.

Taboada, A.C., 2010. Mississsippian-Early Permian brachiopods from western Argentina: tools for middle- to high-latitude correlation, paleobiogeographic and paleoclimatic reconstruction. Palaeogeography, Palaeoclimatology, Palaeoecology, v. 298, p. 152-173.

Taboada, A.C., Shi, G.R., 2009. Yagonia Roberts (Brachiopoda: Chonetidina) from the Maliman Formation, Lower Carboniferous of western Argentina: palaeobiogeographical implications. Alcheringa, v. 33, p. 223-235.

Thomas, G.S.P., and Connell, R.J., 1985. Iceberg drop, dump, and grounding structures from Pleistocene glacio-lacustrine sediments, Scotland. Journal of Sedimentary Petrology, v. 55, p. 243-249.

Woodworth-Lynas, C.M.T., and Dowdeswell, J.A., 1994. Soft-sediment striated surfaces and massive diamicton facies produced by floating ice. In: Deynoux, M., Miller, J.M.G., Domack, E.W., Eyles, N., Fairchild, I.J., and Young, G.M. (Eds.) Earth's Glacial Record, Cambridge University Press, Cambridge, p. 241-259.

Figure Captions

Figure 1: Paleogeographic reconstruction of the southwestern margin of Gondwana (ca. 320 Ma). Major late Paleozoic depositional basins of South America (SA) are highlighted in dark gray. Plate reconstruction from Isbell et al., 2012 (and refs therein). South Polar Circle and S50º latitude line for 320 Ma are shown for reference, based on polar wander path from Domeier et al., 2011. ANT=Antarctica, AFR=Africa

Figure 2: A) ETM+ (Enhanced Thermatic Mapper Plus) image of the study area (NASA, 2002). Major tectonic regimes, Cuyania domain and Precordillera domain are referenced (sensu Limarino et al., 2006). B) Regional map of the study area in Argentina and South America. C) Geologic map of the study area (inset in A) after Gulbranson (2011). Black circles denote sample localities for radiometric ages (Gulbranson et al., 2010). D) General stratigraphic column of the Río Blanco Basin, stratigraphic contacts are dated by (1) Gulbranson et al. (2010) and (2) Pere-Loinaze et al. (2010).

Figure 3: A) Google Earth image of the study area. Numbered bars correspond to sections measured in the study. The white line denotes the contact between the Punta del Agua

and Río del Peñon fms. Note the thinning of the Lower Río del Peñon Fm. between sections 3 and 4. B) Cross-section of the study area focusing on the basal diamictites of the Lower Río del Peñon Fm. Numbered bars correspond to the sections in A. The blue interval denotes diamictite that does not display evidence of internal deformation. The red interval indicates the approximate thickness and continuity of internally deformed diamictite.

Figure 4: Contact of the Punta del Agua and Río del Peñon fms. A) Paleovalley geometry of the contact between the Punta del Agua and Río del Peñon fms. Photograph was taken facing the western limb of the syncline near route 76 (modified from Gulbranson et al., 2010). B) Photograph of the contact between the Punta del Agua and Lower Río del Peñon fms. at section 4. The contact trends upsection through the basal diamictite towards the south (ridgeline). The lowermost diamictite at the contact displays curvilinear grooves interpreted as iceberg-keel marks.

Figure 5: Photographs of iceberg keel marks. A) Iceberg keel marks, curvilinear grooves, exposed on a bedding plane at section 4. Grooves transition laterally into unmodified sediment (arrows). B) Close-up of iceberg keel marks in (A).

Figure 6: Stratigraphic columns from sections 1, 2, and 3 of the Lower Río del Peñon Fm. and the lowermost sandstone of the Middle Río del Peñon Fm. The blue interval denotes diamictite that does not exhibit evidence of internal deformation. The red interval denotes diamictite that is internally deformed. The green interval highlights delta plain facies in

between the glacigenic diamictites and the overlying erosional contact with the Middle Río del Peñon Fm. Sandstones of the Middle Río del Peñon Fm. are channelized and channel stacking density decreases towards section 1.

Figure 7: Photograph (left) and interpretation (right) of the Lower Río del Peñon Fm. diamictites at section 3. Note the change in dip angle between the basal-most diamictite (blue color) and the overlying deformed diamictites (red color) that are interpreted to be three separate slump blocks. Bedding geometry is highlighted in the interpretation diagram to illustrate folding. The measured shear direction of slump 2 is 163º, the general strike of the outcrop is 195º. Green and yellow colors indicate delta plain facies of the Lower Río del Peñon Fm. and the Middle Río del Peñon Fm., respectively.

Figure 8: Photograph (A) and interpretation (B) of sandstone 'micro thrusts' in section 3 beneath slide block 2. B) Red sandstone forms an en echelon pattern with underlying green sandy siltstone interbedded. Note that the middle red sandstone protrudes into the overlying finely bedded sandstone and warps the bedding. Inferred glide planes (arrows) have an orientation of 163º.

Figure 9: Photograph (left) and interpretation (right) of the Lower Río del Peñon Fm., diamictites at section 4. The underlying diamictite (blue) wraps around slide 1 and bedding displays a subvertical orientation on the southeastern side of slide 1 (facing uphill). Diamictites 1 and 2 do not display evidence of internal deformation and show a bedding contact concordant with bedding geometry in the overlying Middle Río del

Peñon Fm. These deposits likely formed from suspension settling of meltwater plumes and emplacement of iceberg-rafted debris. Interbedded sandstone in slide 2 (green color) is truncated and offset and displays back-tilting. Bedding is highlighted by black lines, note the lines in slide 2 define thrust faults and reverse faults.

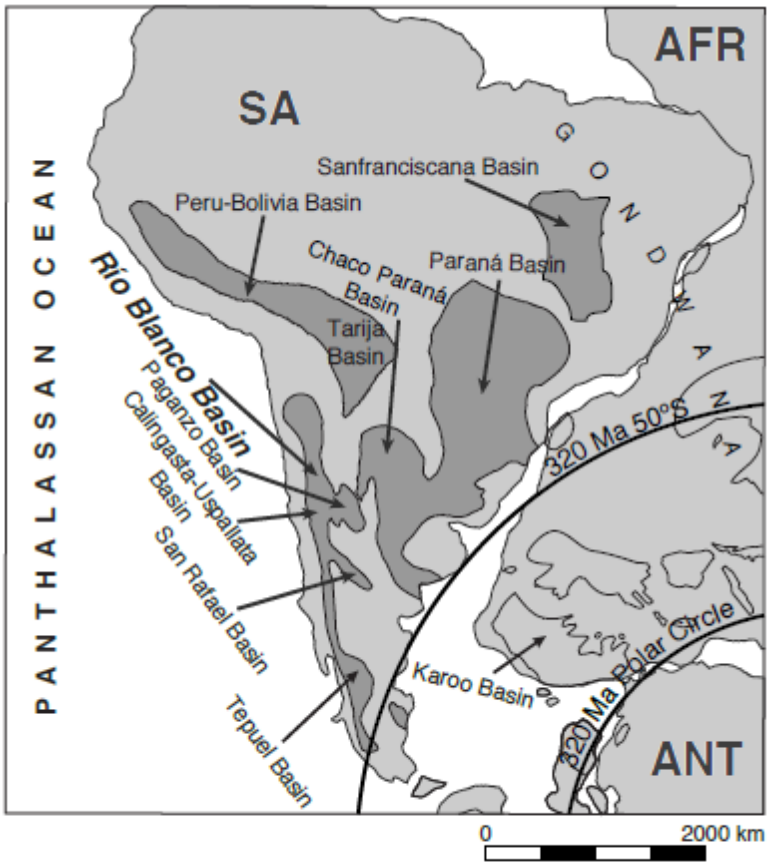

Figure 1.

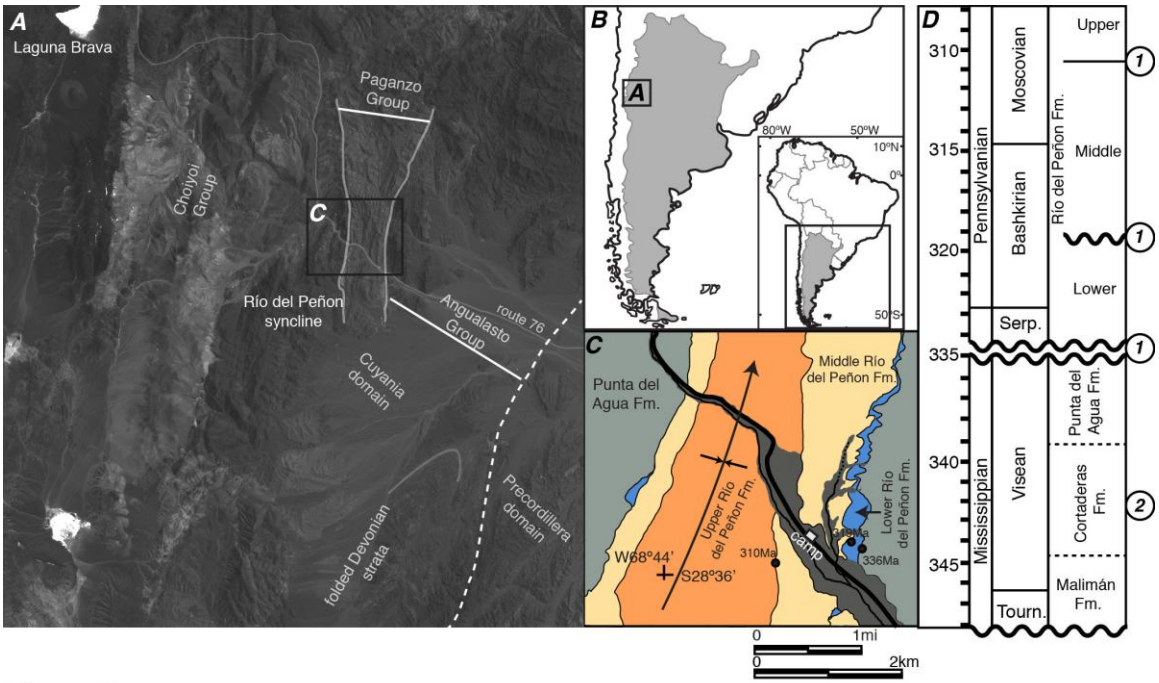

Figure 2.

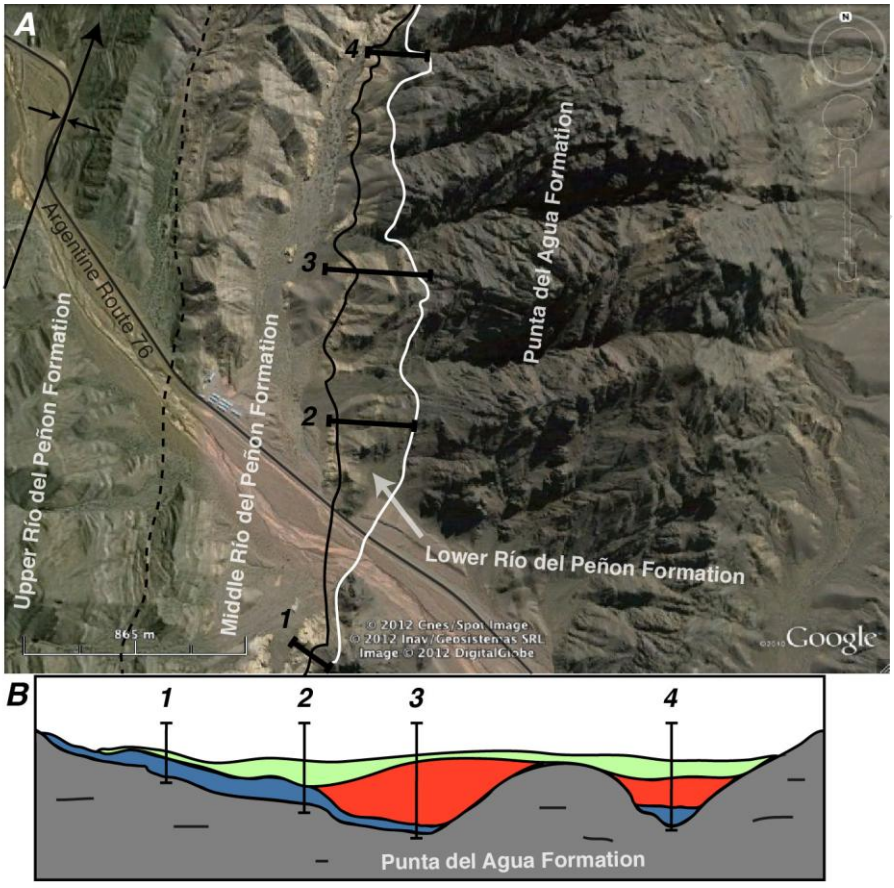

Figure 3.

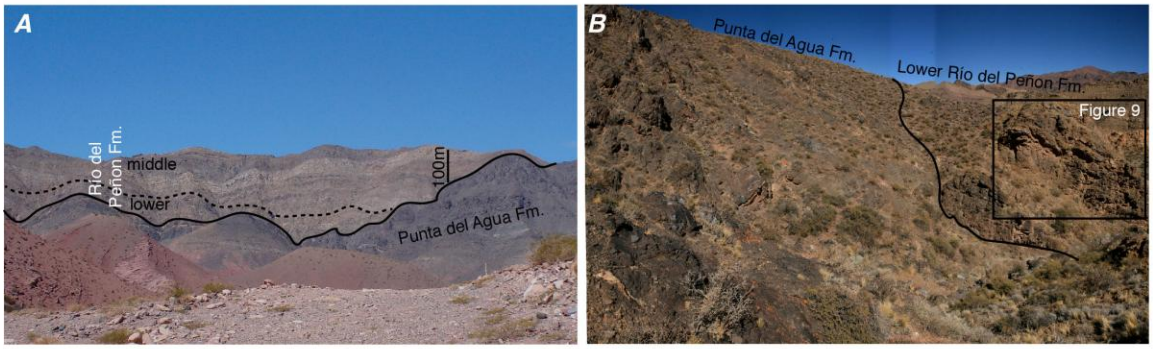

Figure 4.

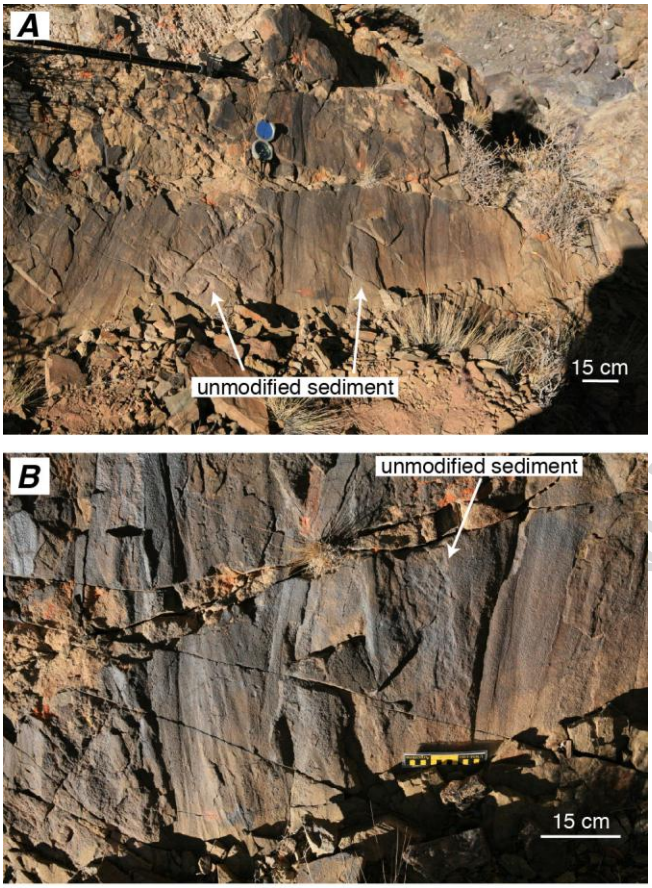

Figure 5.

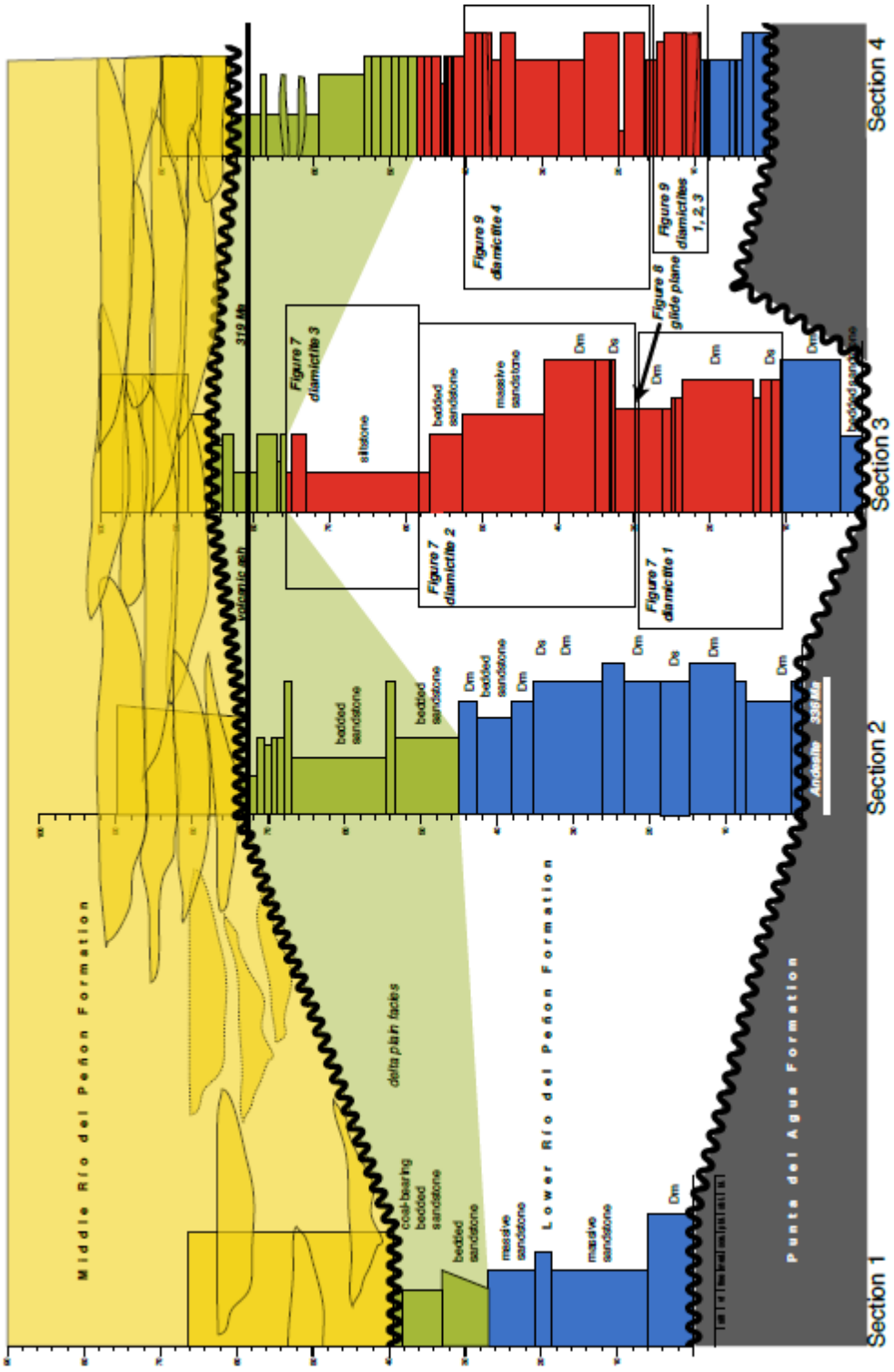

Figure 6.

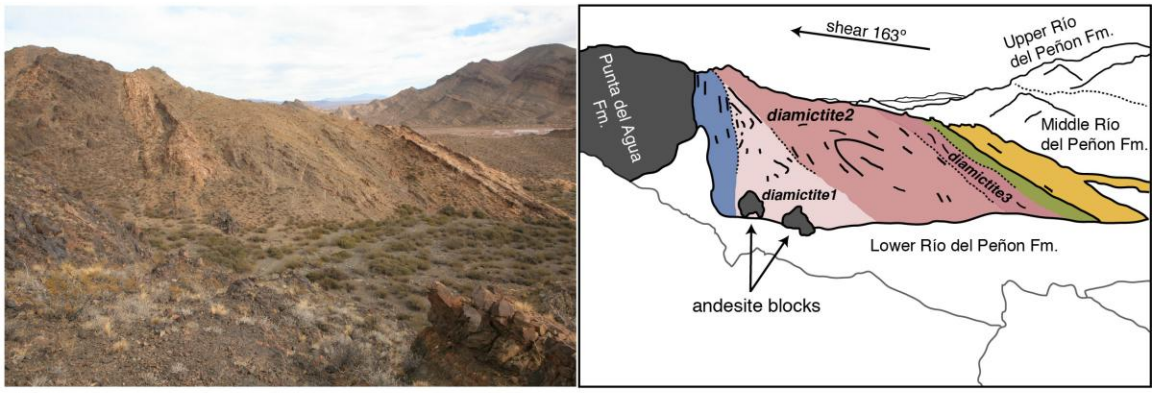

Figure 7.

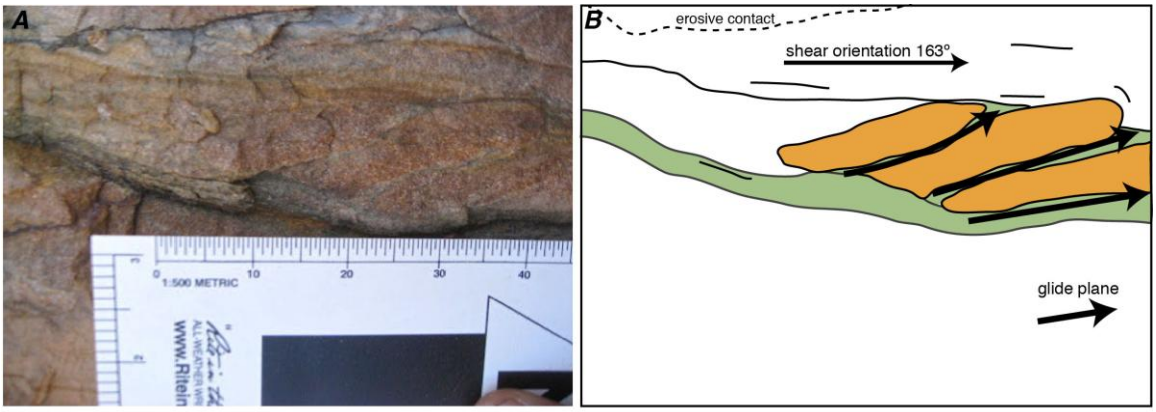

Figure 8.

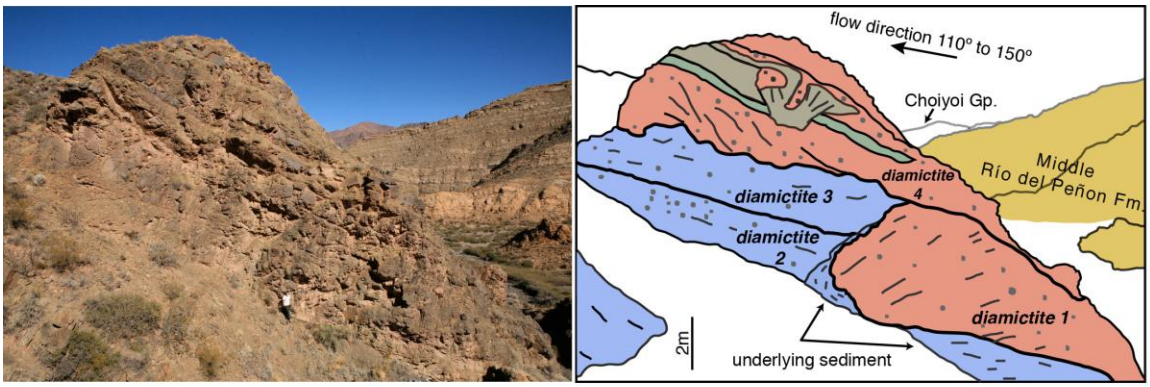

Figure 9.

Table 1: Comparison of contemporaneous mid-Carboniferous diamictites of South America to diamictites of the Río Blanco Basin

Reference	Location	Sedimentary Features	Environment of Deposition	Inferred ice direction/ice volume?
Gonzalez-Bonorino, 1992	Tepuel Basin	Massive, chaotic, laminated, and thin-bedded diamictites, mudstone with outsized clasts	Glacier grounded below sea-level, gradual sedimentation from floating ice or melt water plume (massive diamictite), deposition at the grounding line (chaotic diamictite) with mass transport, mass transport deposits (laminated and thin-bedded diamictites)	Western sediment transport direction from Patagonian highlands
Espejo and Lopez-Gamundi, 1994	San Rafael Basin	Sandstone, shale, diamictite	Glacial marine (diamictite), pro-delta, delta-front (shales and sandstones), mouth-bar (sandstones)	N/A
Henry et al., accepted (this volume)	San Rafael Basin	Mudstone, sandstone, diamictite, deformed diamictite	Marine (mudstone), deltaic (sandstone), wet-based tidewater glacier (diamictite, stratified diamictite, deformed diamictite)	Alpine glaciers, sediment transport direction SE-NW from the Patagonian Massif
Lopez-Gamundi, 1987; Lopez-Gamundi et al., 1992	Tarija, Calingasta-Uspallata & Paganzo basins	Tarija Basin: soft-sediment deformation, well-sorted sandstone lenses in massive matrix-supported diamictite; Calingasata-Uspallata & Paganzo basins: Tillites, fine-grained laminated diamictites, matrix-supported diamictite, boulder pavement, pebbly shale	Tarija Basin: alluvial deposition, pro-delta, delta-slope, and delta-plain deposits; Calingasta-Uspallata & Paganzo basins: ice contact glaciomarine system with gravity flow deposits, subglacial flow tills, shelf sedimentation with IRDs	N/A
Henry et al., 2008; 2010	Calingasta-Uspallata & Paganzo basins	Clast-poor and clast-rich diamictite, massive and weakly stratified diamictite, bedded diamictite, folded beds, load structures, dewatering structures	Morainal bank complex from a wet-based tidewater glacier: rain-out from glacial meltwater plumes and debris flows (massive diamictite), settling of sediment from melt water plumes with IRDs (stratified diamictite), debris flows (bedded diamictite)	NE-SW
Lopez-Gamundi and Martinez, 2000	Calingasta-Uspallata & Paganzo basins	Diamictite, pebbly shale, striated boulder pavement	Subglacial environment (boulder pavement), glacimarine environment (pebbly shale, diamictite)	N-NE, regional slope to the north into embayment and full marine environments
Dykstra et al., 2006; Kneller et al., 2004	Paganzo Basin	Folded/sheared diamictite, rafted blocks, sandstone, shale, siltstone	Fjord setting, isce-contact delta, deep-water lacustrine environment, turbidity currents. Mass transport deposition of basal diamictite	N/A
Buatois and Mangano, 1995	Carboniferous Lake Malanzan, eastern Paganzo Basin	Mudstone with outsized clasts, ripple-laminated sandstone and siltstone, massive sandstone, folded sandstone, wave-ripple laminated sandstone	Underflow currents in lacustrine basin with IRDs (mudstone and outsized clasts), turbidity currents (ripple-laminated and massive sandstone), slumps in delta lobe (folded sandstone), wave reworking of turbidity current deposits (wave-rippled sandstone)	N/A
Marenssi et al., 2005; Perez Loinaze et al., 2010	Paganzo Basin	Clast-poor massive diamictite, rhythmites, laminated pebbly mudstone and shale, stratified diamictite, shale	Grounding line system in a low-relief glacimarine environment: morainal bank, bank-core, and bank-back; several episodes of glacial advance and glacial retreat	Provenance analysis suggests east-west glacier advance
Limarino et al., 2010	Northernmost Paganzo Basin	Monomictic diamictites, polymictic diamictites, shale-sandstone cycles, shales	Resedimented diamictite in high energy environment, fjord development (shale-sandstone, shale)	N/A
Rocha-Campos,	Paraná Basin	Massive diamictite, striated and	Temperate, warm-based,	SE-NW

2008		polished surfaces, discontinuous and foliated diamictite	tidewater glaciers extending westward from Namibian highlands, mass flow deposition, underflow currents with IRDs	
This study	Rio Blanco Basin	Massive diamictite, stratified diamictite, grooved sediment, decimeter-scale folds, meter-scale thrusts, sheared zones, ripple laminated sandstone	Resedimented diamictite over irregular topography	Mass flow direction is from NE-SW suggesting a distinct ice volume from the proto-Precordillera

Studies are listed relative to depositional basin from south to north
*IRD = ice-rafted debris

Table 2: Literature summary of sedimentologic and stratigraphic results from the Río Blanco Basin

Sedimentary Features	Summary of Results	Reference
Fluvial sandstones, marine shales and sandstones, excluding basal diamictites	Description of the Rio del Peñon Fm. as fluvial, paralic, and marine stratigraphy, Permian in age	Scalabrini Ortiz, 1972; Scalabrini Ortiz and Arrondo, 1973; Limarino et al., 1996
Volcaniclastic deposits, sandstones, shales	Interpreted the Punta del Agua and Rio del Peñon fms as the youngest tectonosedimentary cycles in the region	González and Bossi, 1986
Invertebrate fauna of Rio del Peñon Fm.	Temperate fauna, distinct from cold water fauna in southern basins (Tepuel), affinities with tropical assemblages	González, 1989; 1993; 1997
Conglomerate, cross-bedded sandstone	Defined the Angualasto Gp. as the oldest tectonosedimentary cycle in the region, interpreted fluvio-deltaic and marine environment of deposition	Limarino and Cesari, 1993
Palynology	Documented 21 fossiliferous horizons in the lower Río del Peñon Fm., and 2 fossiliferous in the middle and upper Río del Peñon Fm. Define Upper Carboniferous-Lower Permian age range for Río del Peñon Fm.	Gutiérrez and Limarino, 2006
Basal diamictites of Rio del Peñon Fm.	First documentation of glacigenic diamictites in the lower Rio del Peñon Fm.	Gulbranson et al., 2008; Ezpeleta and Astinia, 2008
Volcanic ash, ignimbrite, diamictite, fluvial, paralic, and marine facies of Rio del Peñon Fm.	U-Pb geochronology, inferred duration of unconformities, revised stratigraphic age range for Rio del Peñon Fm. to Serpukhovian-Asselian and Punta del Agua Fm. to the Visean.	Gulbranson et al., 2010
Diamictite	Oldest glacigenic sediments in the Rio Blanco Basin are Visean in age (Cortaderas Fm.), revised interpretation of climate from endemic paleoflora	Perez Loinaze et al., 2010

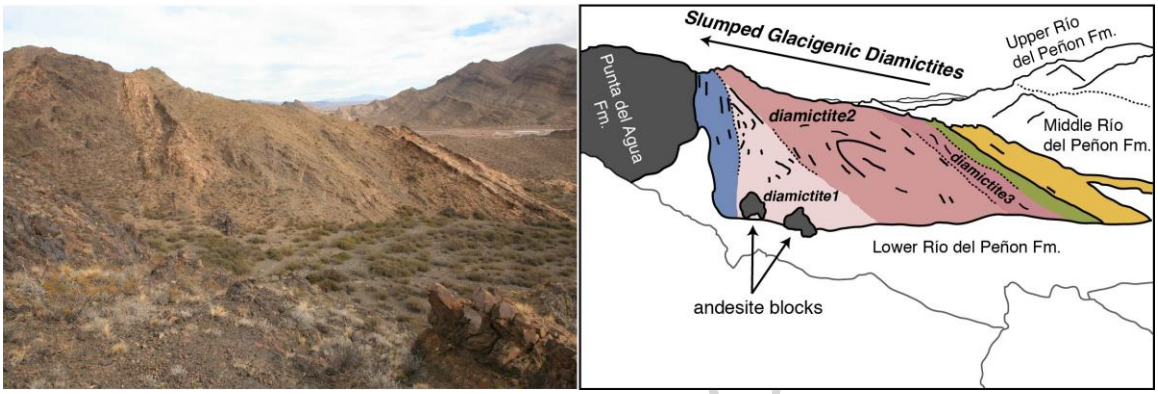

Graphical abstract

Highlights

- Low reliability of slumped glacigenic diamictite for ice volume reconstruction
- Meter-scale deformation is described and interpreted in the diamictite succession
- The occurrence of mass transport deposits suggests tectonic control on glaciation